

Research article

Fabrication of Nanoporous Fe₃O₄-Fe₂O₃/Fe composites by anodization at a safety voltage of 30 V and heat treatment of electroformed Fe foils

Chang-Wei Su^{a, b, *} Wei Yang^{a, b}, Lin-Xing Zhou^{a, b}, Guang-Can Wang^c, Jun-Min Li^{a, b}, Li-Li Feng^{a, b}, Jun-Ming Guo^{a, b}, Ying-Jie Zhang^{a, b, **}

^a Key Laboratory of Chemistry in Ethnic Medicinal Resources, State Ethnic Affairs Commission & Ministry of Education, Yunnan University of Nationalities, D-306, Guang-Jing Compound, Kunming 650500, PR China

^b Engineering Research Center of Biopolymer Functional Materials of Yunnan, Yunnan University of Nationalities, Kunming 650500, PR China

^c Center of Modern Analysis and Test, Yunnan University, Kunming 650091, PR China

Abstract

The formation of nanoporous anodic film on an electroformed Fe foil surface is investigated in ethylene glycol solution containing 0.1 M NH₄F and 2.5 vol % H₂O at a safety voltage of 30 V by electrochemical anodization. A nanoporous array, whose pores are ~35 nm in size, can be formed after anodization for 30 min. The nanopores become big and irregular with the anodization time. Structural retention of the nanoporous array is achieved upon annealing in air at 400 °C for 1 h. The X-ray diffraction (XRD) and energy dispersive X-ray spectroscopy (EDS) patterns suggest that the nanoporous anodic film is amorphous and transforms to a Fe₃O₄-Fe₂O₃ mixture after annealing in air at 400 °C for 1 h. The electrochemical properties of the nanoporous Fe₃O₄-Fe₂O₃/Fe composite anodes for Li-ion batteries are evaluated by means of cyclic voltammograms and charge/discharge curves. The results indicate that the nanoporous Fe₃O₄-Fe₂O₃/Fe composite exhibited different electrochemical performances, such as a low initial discharge voltage plateau at 0.65 V. The discharge capacity is up to 2.2 mA h at the first cycle and 0.51 mA h at the 50 th cycle.

Keywords: Anodization; Nanoporous; Iron foil; Lithium ion battery

* Corresponding author. Tel./fax: +86 871 5910017, Fax: +86 871 5910014

** Corresponding author. (Y.-J. Zhang)

1. Introduction

Nanostructural iron oxides have been widely studied as anode materials for lithium-ion batteries (LIBs) [1-14], due to high theoretical capacity (for example Fe_3O_4 , 926 mA h g^{-1}), non-toxicity and low cost. They can be obtained by solvothermal syntheses [12-14], template replication [15, 16] and electrochemical anodization [17-27]. Amongst these methods, the electrochemical anodization is readily to form nanotubular [17-20] or nanoporous [21-24] iron oxides films on Fe foils. For example, rugated porous Fe_3O_4 films on Fe foils, exhibiting a high cycling stability, have been synthesized by the electrochemical anodization [22]. Anodization of Fe foils is usually carried out in ethylene glycol (EG) electrolytes containing NH_4F and H_2O at a higher voltage than the safety voltage of 36 V. For examples, nanotubular iron oxides can be obtained in the EG electrolytes at 50 V [17-20] or at 40 V if the iron surface is electropolished [19], while nanoporous iron oxides are formed at higher voltages [21, 22]. Naturally, the transition voltage from nanotubular structure to nanoporous structure can be affected by water and fluoride concentrations in EG electrolytes, and other anodizing parameters (such as pH and temperature) [19, 23, 24]. Other fluoride-organic electrolytes have been also used to fabricate nanostructured anodic films on Fe foils [25-27], but the applied voltage is still high (>36 V).

For operational safety, it is desirable for anodization of Fe foils to obtain nanostructural iron oxides at a safety voltage (<36 V). In this study, the anodization behaviors of electroformed Fe foils are investigated in a EG electrolyte containing 0.1 M NH_4F and 2.5 vol % H_2O , and a nanoporous array anodic film can be prepared at a safety voltage of 30 V. The iron anodic films consist mainly of trivalent iron species (for example FeOOH [21, 22]) containing some impurities of fluorides and oxyhydroxides [19-24]. They can transform to Fe_2O_3 with the same nanostructures of anodic films after annealing in inert, oxygenous [18, 20, 26, 28] or hydric [17, 18] atmospheres below 550 °C. But Cheng et al [22] demonstrated that rugated porous Fe_3O_4 films are prepared by annealing of porous anodic films on Fe foils in an atmosphere of Ar/H_2 (5 vol % H_2). Due to high electrical conductivity of Fe_3O_4 , it is regarded as one of the most promising anode materials for lithium-ion batteries [22]. However, in this study, a Fe_3O_4 - Fe_2O_3 mixture is obtained after annealing in air at 400 °C for 1 h. Thereby, we demonstrate that nanoporous Fe_3O_4 - Fe_2O_3 /Fe composite foils are fabricated by anodization of electroformed Fe foils in a EG electrolyte containing 0.1 M NH_4F and 2.5 vol % H_2O at a safety voltage of 30 V and further annealing in air at 400 °C for 1 h. The electrochemical performances of the nanoporous Fe_3O_4 - Fe_2O_3 /Fe composite anodes for Li-ion batteries are studied.

2. Experimental

2.1 Chemicals and materials

Fe foils with a purity of 99.9 wt% and a thickness of $60 \pm 5 \mu\text{m}$ were prepared by galvanostatic electrodeposition (25 A dm^{-2}) in a Fe + Fe bath [28]. A structure of polygonal crystal of the Fe foils is presented in Fig. 1 a. An EG electrolyte containing 0.1 M NH_4F and 2.5 vol % H_2O were prepared using analytic grade chemicals and deionized water to study anodization of the Fe foils.

2.2 Fabrication of nanoporous Fe_3O_4 - Fe_2O_3 /Fe foils

The anodization of Fe foils ($30 \times 50 \text{ mm}$) was carried out at 10-30 V for 10-60 min by exposing only one

surface to the EG electrolyte and masking the other surface using an insulating tape. A pure Ti plate (25 × 50 mm) was used as the counter electrode. The distance between Fe foils and the Ti plate was kept at 10 mm. During anodization, the electrolyte was stirred at about 300 rpm with a 27 mm magnetic bar at ambient temperature. After anodization, the samples were rinsed thoroughly with deionized water and ethanol, and then dried by hot wind before further processing. Morphology of Fe foils anodized at 30V is shown in Fig. 1 b. It is observed that the shape of crystal of Fe is retained, although grain boundaries and edges of polygonal crystals of Fe are corroded to be many gaps. The morphology can be also retained after annealing in air at 400 °C for 1h, as Fig.1 c shown.

2.3 Characterization of nanoporous Fe₃O₄-Fe₂O₃/Fe foils

The surface morphologies of all samples were characterized by scanning electron microscopy (SEM, QUANTA 200, America FEI), and the elemental composition was estimated by energy dispersive X-ray spectroscopy (EDS). The X-ray diffraction (XRD) patterns were recorded using a D/max-TTRIII diffractometer with Cu Ka radiation over 2θ-range of 35-120°.

The electrochemical performance was evaluated using CR2025 coin-type cells. The Fe₃O₄-Fe₂O₃/Fe composite foils were cut into disks with a diameter of 1.6 cm (2.0 cm²) and regarded as working electrode. Lithium foil was used as both counter and reference electrodes. The electrolyte was 1M LiPF₆ in ethylene carbonate (EC) and dimethyl carbonate (DMC) (1:1 by volume). Cyclic voltammetry (CV) was performed on the electrochemical workstation (IM6ex, ZAHNER-elektrik GmbH & Co. KG, Germany) in a potential range of 0.01-3.00 V (vs. Li⁺/Li) at a scan rate of 0.4 mV s⁻¹. The discharge/charge measurements were carried out using the Land battery system (CT2001) at a constant current of 0.5 mA in a potential range of 0.01-3.00 V (vs. Li⁺/Li).

3. Results and discussion

3.1 Anodization of Fe foils

Fig. 2 shows the change in the surface morphology of the samples anodized for 30 min with anodizing voltage. It is found that the pore formation gradually become a main process when the applied anodizing voltage increases. At 30V, a nanoporous array with the pore diameter of ~35 nm is formed. However, such array needs a voltage of over 40 V in literatures [21, 22]. At lower voltages (10 and 20 V), numerous blocks with different shapes and sizes on the surface of polygonal crystals of Fe are presented as Fig. 2 a and b shown, due to asymmetrical corrosion or dissolution of Fe.

The effect of anodization time on the surface morphology of the samples anodized at 30 V is shown in Fig. 3. The color of anodic films can be visible to the naked eye, changing from orange to brown with increasing anodization time (See Figure S1 shown in Supporting Information). The morphology of Fe foils anodized at 30 V for 10 min is shown in Fig. 3 a, while Fig. 3 b shows the morphology of a sample anodized at the same voltage for 60 min. It can be seen from Fig. 3 a that the porous nature of the anodic film is revealed after anodizing for 10 min, although the pores are smaller and not uniform in size than that of 30 min (Fig. 2 c). The pores become wide to ~120 nm at 60 min as shown in Fig. 3 b, where many fine pores are observed at their bottoms (see the inset shown in Fig. 3 b). The result should be associated with chemical dissolution of anodic films [23] and oxygen bubble dwelling on the films during anodization.

Fig. 4 a shows a cross section of an anodic film on Fe foil obtained at 30 V for 30 min. It is obvious to be a bilayered structure. The thickness of the anodic film is approximated to be 2.5 μm . Fig. 4 b discloses the presence of lots of cylindrical pores, which are aligned approximately normal to the crystal surface of Fe and consequently whose direction changes nearby grain boundaries of Fe crystals.

Fig. 5 shows a SEM image of a sample anodized at 30 V for 30 min and subsequently annealed at 400 $^{\circ}\text{C}$ for 1 h. The surface color of the sample becomes crimson-black (see Fig. S1. e). It can be seen from Fig. 5 that the nanoporous array has been retained. Comparing Fig. 5 a with Fig. 2 c and Fig. 5 b with Fig. 4 b, it is found that the pores become smaller ($\sim 25\text{nm}$) after annealing. This phenomenon of pore filling has been also observed on the samples with a long annealing period by Prakasam et al [26].

3.2 EDS and XRD

Fig. 6 shows the EDS spectra of the samples anodized at 30 V for 30 min before and after annealing at 400 $^{\circ}\text{C}$ for 1 h. Fe, O and Au are main three elements. The Au element came from sputtered Au before detection. The corresponding XRD patterns of above two samples are shown in Fig. 7. No diffraction peaks except that of Fe (JCPDS PDF no. 06-0696) are observed from Fig. 7 a, indicating that the anodic film is amorphous. The amorphous anodic films of Fe have been also found by many researchers [20, 26, 28]. The XRD pattern shown in Fig. 7 b indicates that a mixture of magnetite (Fe_3O_4) and hematite (Fe_2O_3) is formed after annealing in air at 400 $^{\circ}\text{C}$ for 1h. Hence, we demonstrate that nanoporous $\text{Fe}_3\text{O}_4\text{-Fe}_2\text{O}_3/\text{Fe}$ composite foils are fabricated by anodization and subsequent heat treatment.

3.3 Electrochemical properties of nanoporous $\text{Fe}_3\text{O}_4\text{-Fe}_2\text{O}_3/\text{Fe}$ composite foils

The electrochemical behavior of the nanoporous $\text{Fe}_3\text{O}_4\text{-Fe}_2\text{O}_3/\text{Fe}$ composite foils was evaluated by cyclic voltammetry and discharge/charge cycling. Fig. 8 a shows the galvanostatic charge/discharge curves for a $\text{Fe}_3\text{O}_4\text{-Fe}_2\text{O}_3/\text{Fe}$ composite electrode at a current of 0.5 mA between 0.01 and 3.0 V. The first discharge curve shows a short potential plateau at 0.82 V, a long potential plateau at 0.65 V and then a downward slope until 0.01 V. The discharge plateau between 0.75~0.85 V, being assigned to the formation of Fe and Li_2O , and the downward slope are commonly observed in the first discharge curve for Fe_3O_4 or Fe_2O_3 anodes [29-33], while the discharge plateau at 0.65 V is first observed. The discharge plateau should be ascribed to the structure and composition of the nanoporous $\text{Fe}_3\text{O}_4\text{-Fe}_2\text{O}_3/\text{Fe}$ composite electrode. After the first cycle, the two discharge plateaus disappear, two slopes appear at 1.4-1.0 V and 1.0-0.8V, respectively, and a large capacity loss between the first and second discharge can be observed. The results could be attributed to the formation of a solid-electrolyte interface (SEI) layer on the electrode surface during the first discharge step. As Fig. 8 a shown, the discharge capacity fade from 2.2 mA h at the first cycle to 0.51 mA h at the 50th cycle, indicating that such structural composite material possesses low capacity retention. A main reason should be the part separation between nanoporous $\text{Fe}_3\text{O}_4\text{-Fe}_2\text{O}_3$ films and Fe foils (see Fig. 5 b), which results in peeling off of iron oxides from Fe substrate during discharge-charge cycles. Anchoring fast to iron oxides by growing of metal or conductive polymer nanowires in the cylindrical pores can improve the capacity retention of the nanoporous $\text{Fe}_3\text{O}_4\text{-Fe}_2\text{O}_3/\text{Fe}$ composite anodes. Indeed, the capacity retention was greatly improved when polypyrrole was grown up on the $\text{Fe}_3\text{O}_4\text{-Fe}_2\text{O}_3/\text{Fe}$ by chemical oxidation (see Fig.8 b).

Fig. 8 c shows the CVs of a sample for the initial three cycles in the voltage range from 0.01 to 3.00 V at a scan

rate of 0.4 mV s^{-1} . A sharp reduction peak nearby 0.65 V can be clearly observed in the first cycle, which is consistent with the long discharge plateau at Fig. 8 a. In the second cycle, many cathodic peaks between 1.0 and 0.5 V and an elevating anodic peak centered at 1.78 V suggest that iron oxides discharged partly in the first cycle. Only one wide cathodic peak presents in the potential range from 1.0 to 0.5 V in the third cycle, which is commonly observed in CV curves after the first cycle for Fe_3O_4 or Fe_2O_3 anodes [29-33]. The corresponding anodic peak positively shifts to 1.83 V due to the increase of electrochemical polarization. Two anodic peaks are usually observed between 1.5 and 2.0 V [2, 13, 31-33] even though at a rapider scan rate of 0.5 mV s^{-1} [2], assigning to the oxidation of Fe^0 to Fe^{2+} and Fe^{3+} respectively. But the two anodic peaks are not observed in the CV curves (Fig.8 b). The result suggests that the oxidization of Fe^0 to Fe_3O_4 and Fe_2O_3 should be a one-step reaction. It can be considered that the special structure and composition of nanoporous $\text{Fe}_3\text{O}_4\text{-Fe}_2\text{O}_3/\text{Fe}$ composite electrodes are responsible for the different electrochemical behaviors.

4. Conclusion

In summary, nanoporous $\text{Fe}_3\text{O}_4\text{-Fe}_2\text{O}_3/\text{Fe}$ composite foils have been successfully fabricated by anodization of electroformed Fe foils at 30 V for 30 min and following heat treatment in air at $400 \text{ }^\circ\text{C}$ for 1 h . The XRD and EDS patterns suggest that anodic films are amorphous and transform to a $\text{Fe}_3\text{O}_4\text{-Fe}_2\text{O}_3$ mixture after annealing. The nanoporous $\text{Fe}_3\text{O}_4\text{-Fe}_2\text{O}_3/\text{Fe}$ composite exhibits different electrochemical performances, such as a lower initial discharge voltage plateau at 0.65 V and only one anodic oxidation peak in CV curves. Its capacity retention is not desirable, only 23.2% after 50 cycles. Anchoring fast to iron oxides by growing of polypyrrole can profoundly improve the capacity retention of the nanoporous $\text{Fe}_3\text{O}_4\text{-Fe}_2\text{O}_3/\text{Fe}$ composite anodes.

Acknowledgements

This work was financially supported by the National Natural Science Foundation of China (51062018, 51262031), the Natural Science Foundation of Yunnan (2010FXW004), Program for Innovative Research Team (in Science and Technology) in University of Yunnan Province (2010UY08, 2011UY09), and Yunnan Provincial Innovation Team (2011HC008).

References

- [1] P. Poizot, S. Laruelle, S. Grugeon, L. Dupont, J.M. Tarascon, *Nature* 407 (2000) 496–499.
- [2] B. Wang, J.S. Chen, H.B. Wu, Z.Y. Wang, X.W. (David) Lou, *J. Am. Chem. Soc.* 133 (2011) 17146-17148.
- [3] J.S. Chen, T. Zhu, X.H. Yang, H.G. Yang, X.W. (David)Lou, *J. Am. Chem. Soc.* 132 (2010) 13162-13164.
- [4] M.B. Sassin, A.N. Mansour, K.A. Pettigrew, D.R. Rolison, J.W. Long, *ACS Nano* 4 (2010) 4505-4514.
- [5] B. Jin, A.H. Liu, G.Y. Liu, Z.Z. Yang, X.B. Zhong, X.Z. Ma, M. Yang, H.Y. Wang, *Electrochim. Acta* 90 (2013) 426– 432.
- [6] M. Zhang, M.Q. Jia, Y.H. Jin, *Appl. Surf. Sci.* 261 (2012) 298–305.
- [7] D.Y. Chen, G. Ji, J.Y. Lee, J.M. Lu, *ACS Appl. Mater. Interfaces* 3 (2011) 3078–3083.
- [8] J.P. Liu, Y.Y. Li, H.J. Fan, Z.H. Zhu, J. Jiang, R.M. Ding, Y.Y. Hu, X.T. Huang. *Chem. Mater.* 22 (2010) 212–217.
- [9] J. Zhang, Y. Sun, Y. Yao, T. Huang, A. Yu, *J. Power Sources* 222 (2013) 59-65.
- [10] A.P. Hu, X.H. Chen, Y.H. Tang, Q.L. Tang, L. Yang, S.P. Zhang, *Electrochem. Commun.* 28 (2013)

139–142.

- [11] Q.M. Zhang, Z.C. Shi, Y.F. Deng, J. Zheng, G.C. Liu, G.H. Chen, *J. Power Sources* 197 (2012) 305–309.
- [12] Q.Q. Xiong, J.P. Tu, Y. Lu, J. Chen, Y.X. Yu, Y.Q. Qiao, X.L. Wang, C.D. Gu, *J. Phys. Chem. C* 116 (2012) 6495-6502.
- [13] X.J. Zhu, Y.W. Zhu, S. Murali, M.D. Stollers, R.S. Ruoff, *ACS Nano* 5 (2011) 3333–3338.
- [14] L.H. Duan, Y.D. Huang, D.Z. Jia, X.C. Wang, Z. P. Guo, *Mater. Lett.* 71 (2012) 151-153.
- [15] J.P. Liu, Y.Y. Li, H.J. Fan, Z.H. Zhou, J. Jiang, R.M. Ding, Y.Y. Hu, X.T. Huang, *Chem. Mater.* 22 (2010) 212–217.
- [16] S.B. Ni, D.Y. He, X.L. Yang, T. Li, *J. Alloys Compd.* 509 (2011) L305– L307
- [17] R.R. Rangaraju, A. Panday, K.S. Raja, M. Misra. *J. Phys. D: Appl. Phys.* 42 (2009) 135-303.
- [18] S.K. Mohapatra, S. E. John, S. Banerjee, M. Misra. *Chem. Mater.* 21 (2009) 3048-3055.
- [19] R.R. Rangaraju, K.S. Raja, A. Panday, M. Misra. *Electrochim. Acta* 55 (2010) 785-793.
- [20] T.J. LaTempa, X. Feng, M. Paulose, C.A. Grimes, *J. Phys. Chem. C* 113 (2009) 16293-16298.
- [21] A. Jagminas, K. Mazeika, N. Bernotas, V. Klimas, A. Selskis, D. Baltrunas. *Appl. Surf. Sci.* 257 (2011) 3893–3897.
- [22] H. Cheng, Z.G. Lu, R.G. Ma, Y.H. Dong, H.E. Wang, L.J. Xi, L.X. Zheng, C.K. TSANG, H. Li, C.Y. Chung, J.A. Zapien, Y.Y. Li, *J. Mater. Chem.* 22 (2012) 22692–22698.
- [23] H. Habazaki, Y. Konno, Y. Aoki, P. Skeldon, G.E. Thompson, *J. Phys. Chem. C* 114 (2010) 18853–18859.
- [24] Y. Konno, E. Tsuji, P. Skeldon, G.E. Thompson, H. Habazaki, *J. Solid State Electrochem.* 16(2012)3887-3896.
- [25] A. Jagminas, V. Klimas, K. Mazeika, N. Bernotas, A. Selskis, G. Niaura, *Electrochim. Acta* 56 (2011) 5452-5458.
- [26] H.E. Prakasam, O.K. Varghese, M. Paulose, G.K. Mor, C.A. Grimes, *Nanotechnology* 17 (2006) 4285-4291.
- [27] A. Jagminas, V. Klimas, K. Mazeika, S. Mickevicius, S. Balakauskas, *Appl. Surf. Sci.* 258 (2012) 3321-3327.
- [28] Z. Zhang, M.F. Hossain, T. Takahashi, *Mater. Lett.* 64 (2010) 435-438.
- [29] X. Zhu, W. Wu, Z. Liu, L. Li, J. Hu, H. Dai, L. Ding, K. Zhou, C. Wang, X. Song, *Electrochim. Acta* 95 (2013) 24-28.
- [30] L. Zhang, H.B. Wu, S. Madhavi, H.H. Hng, X.W. Lou, *J. Am. Chem. Soc.* 134 (2012) 17388-17391.
- [31] T. Yoon, C. Chae, Y. K. Sun, X. Zhao, H.H. Kung, J. K. Lee, *J. Mater. Chem.* 21 (2011) 17325-17330.
- [32] H.D. Oh, S.W. Lee, S.O. Kim, J.K. Lee, *J. Power Sources* 244 (2013) 578-580.
- [33] N. Zhao, S. Wu, C. He, Z. Wang, C. Shi, E. Liu, J. Li, *Carbon* 57 (2013) 130-138.

Figure 1

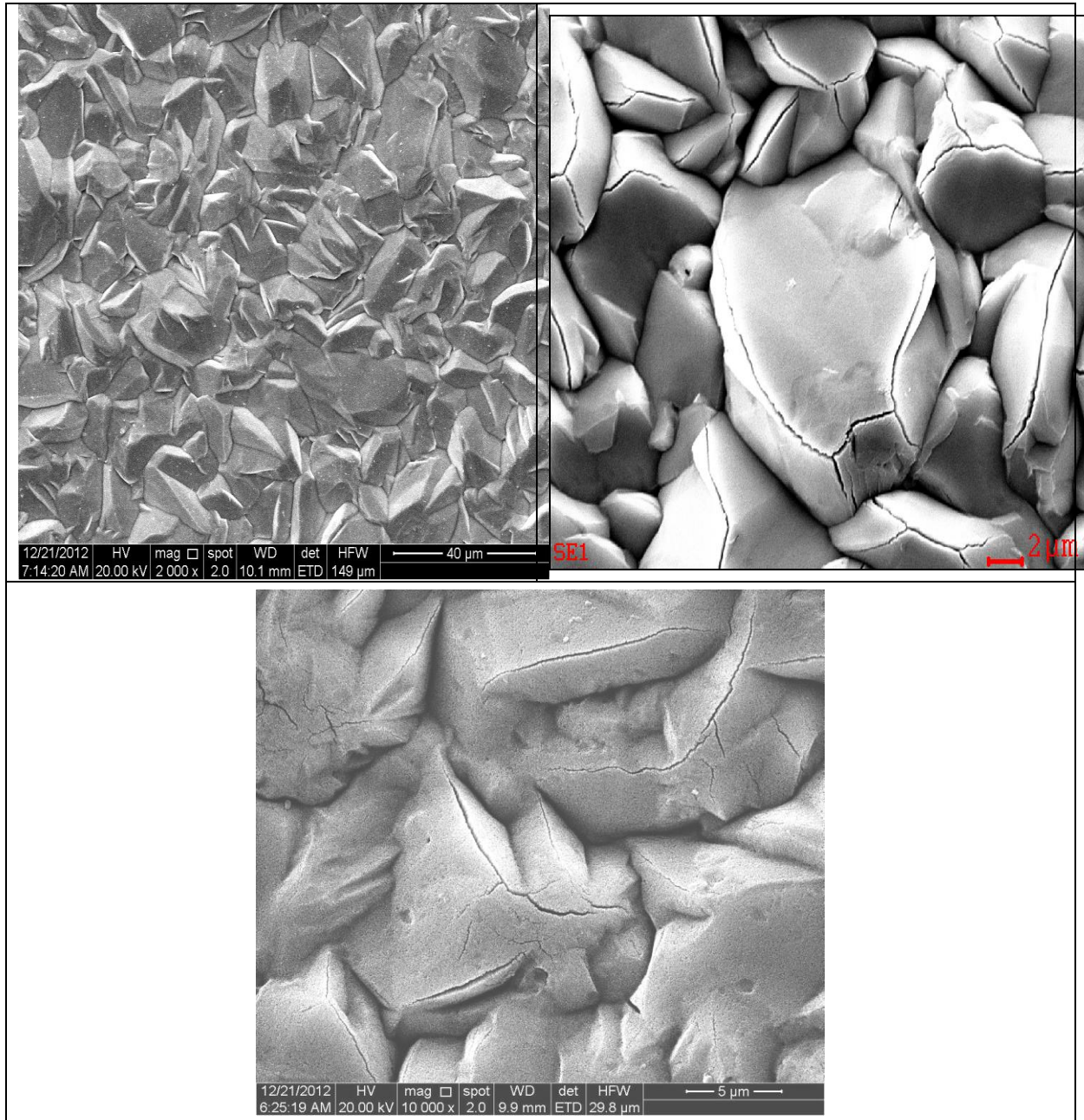


Figure 1: SEM images of iron foil (a) as-electrodeposited, (b) as-anodized and (c) as-annealed

Figure 2

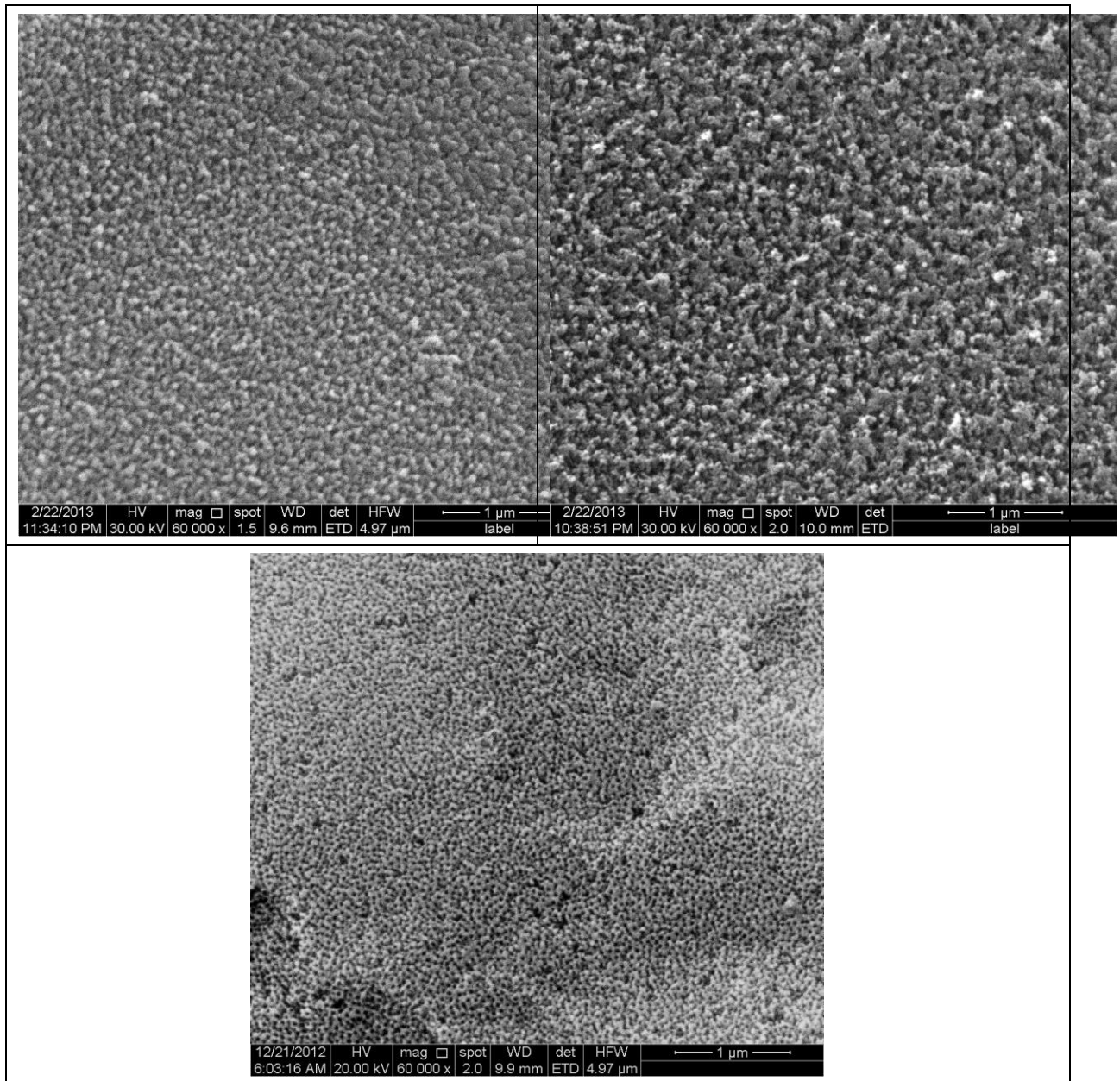


Figure 2: SEM images of surfaces of the Fe foils anodized at (a) 10 V, (b) 20 V and (c) 30V for 30 min

Figure 3

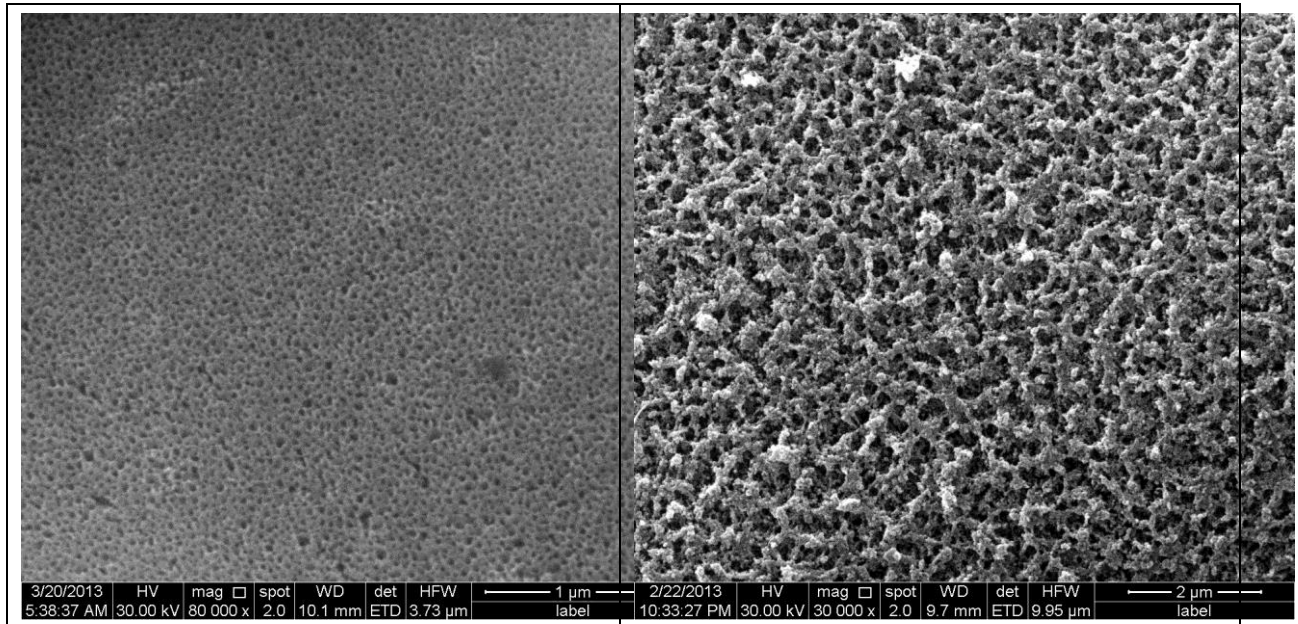


Figure 3: SEM images of Fe foils anodized at 30V for (a) 10 min and (b) 60min

Figure 4

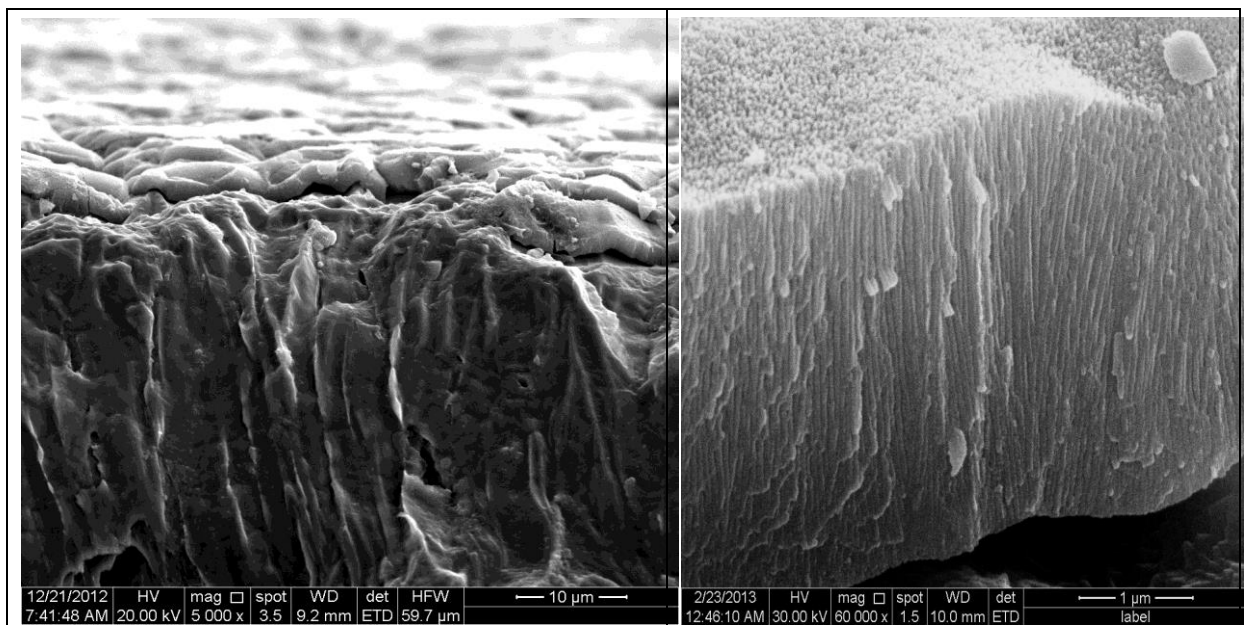


Figure 4: Cross-sectional SEM images of (a) anodic film/Fe foils and (b) anodic film obtained at 30 V for 30 min

Figure 5

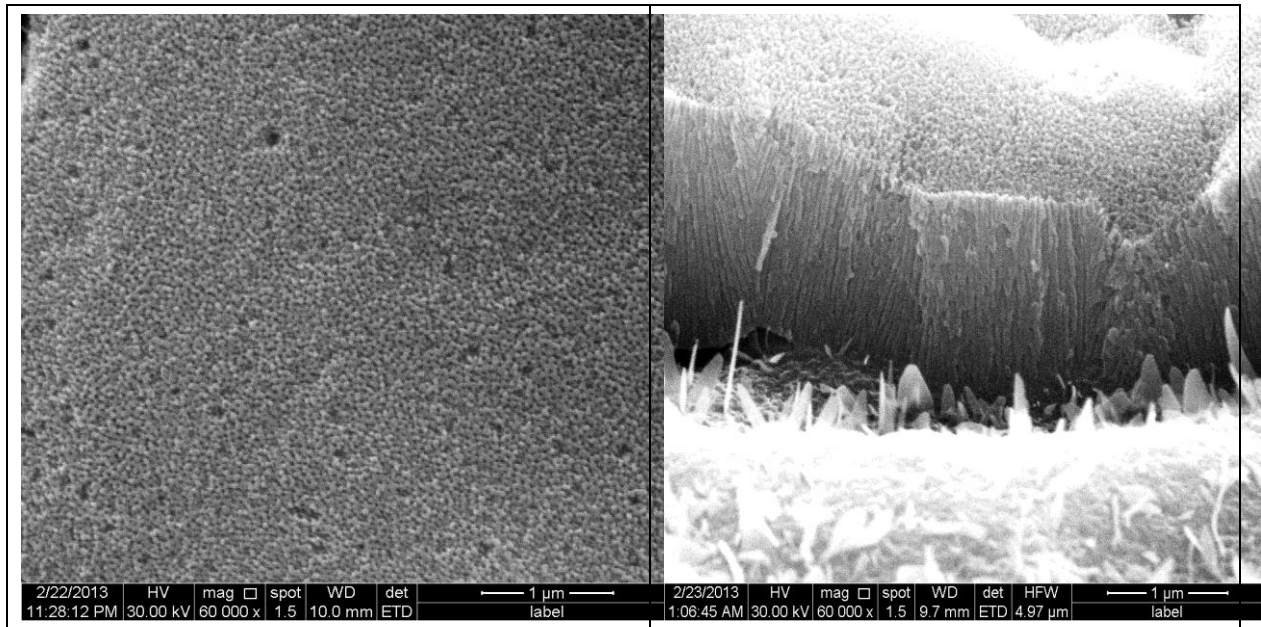


Figure 5: (a) Top view and (b) cross-sectional SEM images of a sample anodized at 30 V for 30 min and subsequently annealed in air at 400°C for 1h

Figure 6

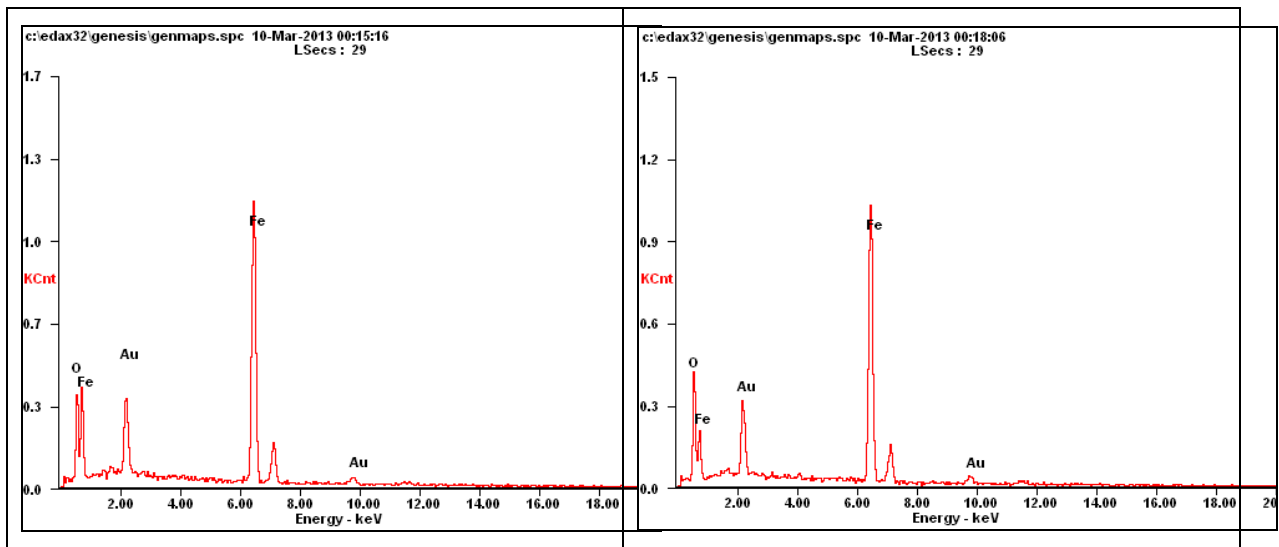


Figure 6: EDS spectra of Fe foils (a) anodized at 30 V for min and (b) subsequently annealed at 400°C for 1 h

Figure 7

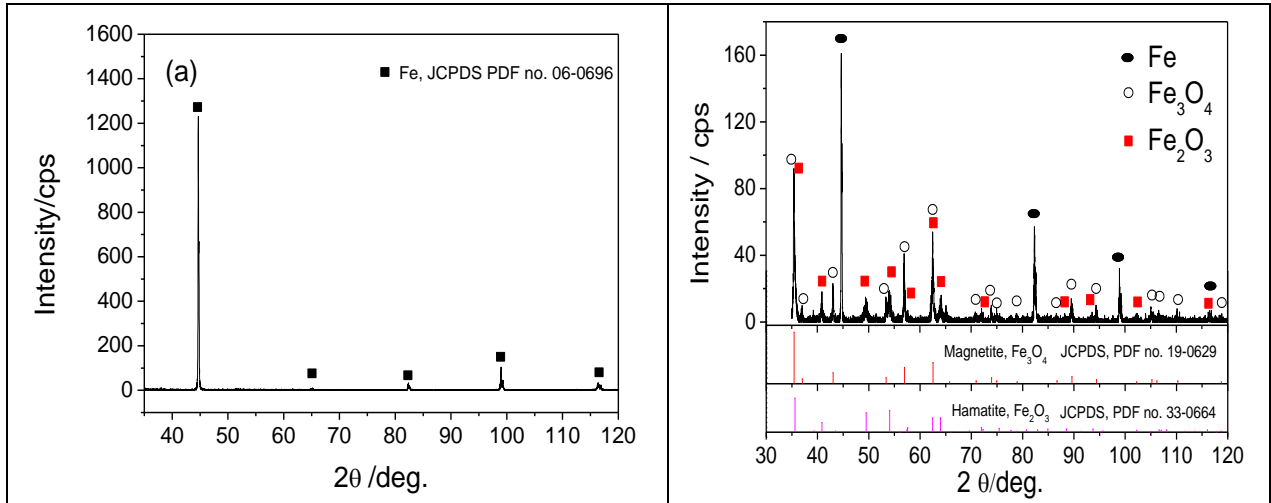


Figure 7: XRD patterns of (a) as-anodized Fe foils and (b) nanoporous $\text{Fe}_3\text{O}_4\text{-Fe}_2\text{O}_3/\text{Fe}$ foils

Figure 8

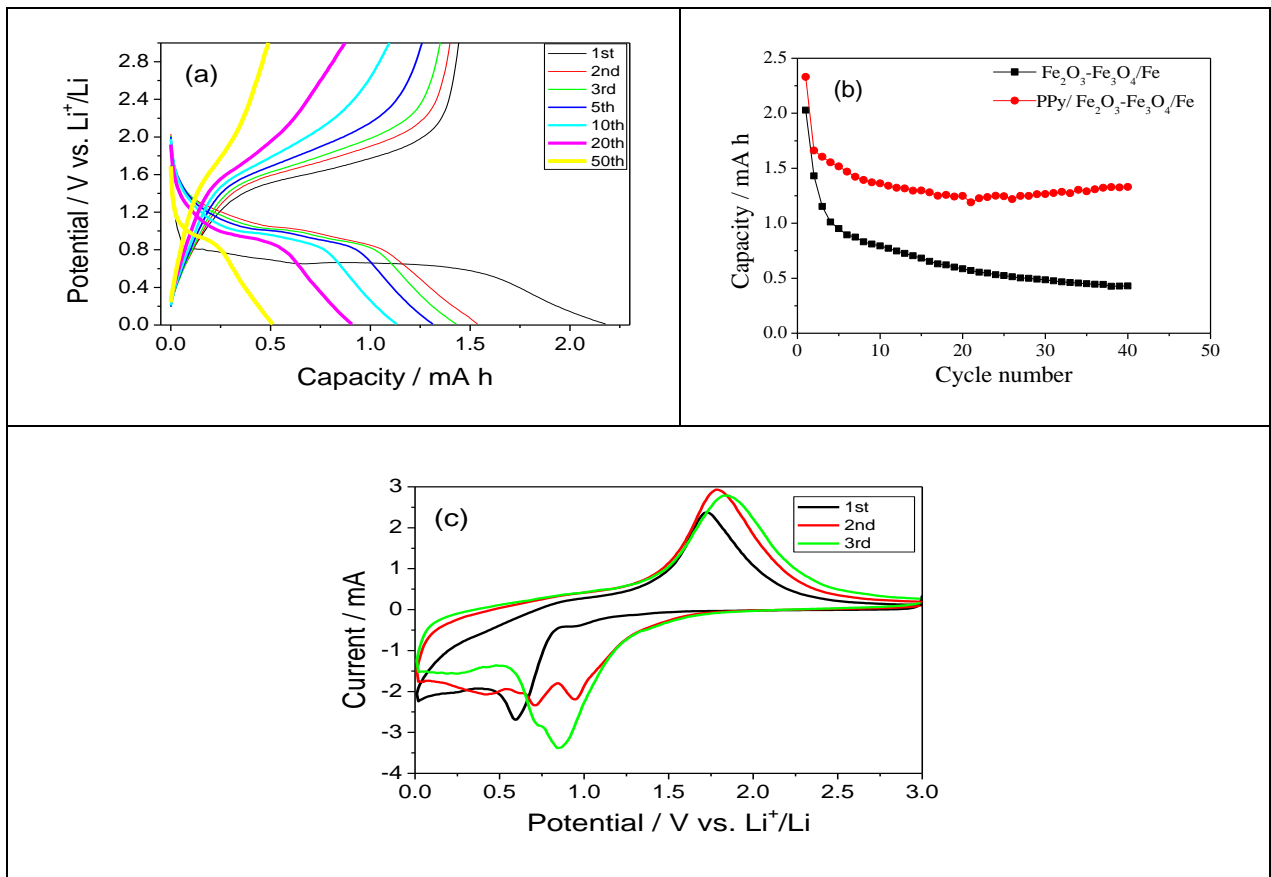


Figure 8: (a) Discharge/charge voltage profiles of a nanoporous $\text{Fe}_3\text{O}_4\text{-Fe}_2\text{O}_3/\text{Fe}$ composite electrode, (b) comparison of capacity retention between with and without polypyrrole, and (c) CV curves between 0.01 and 3.0 V at a scan rate of 0.4 mV s^{-1} of a nanoporous $\text{Fe}_3\text{O}_4\text{-Fe}_2\text{O}_3/\text{Fe}$ composite electrode

Supporting Information

Figure S1

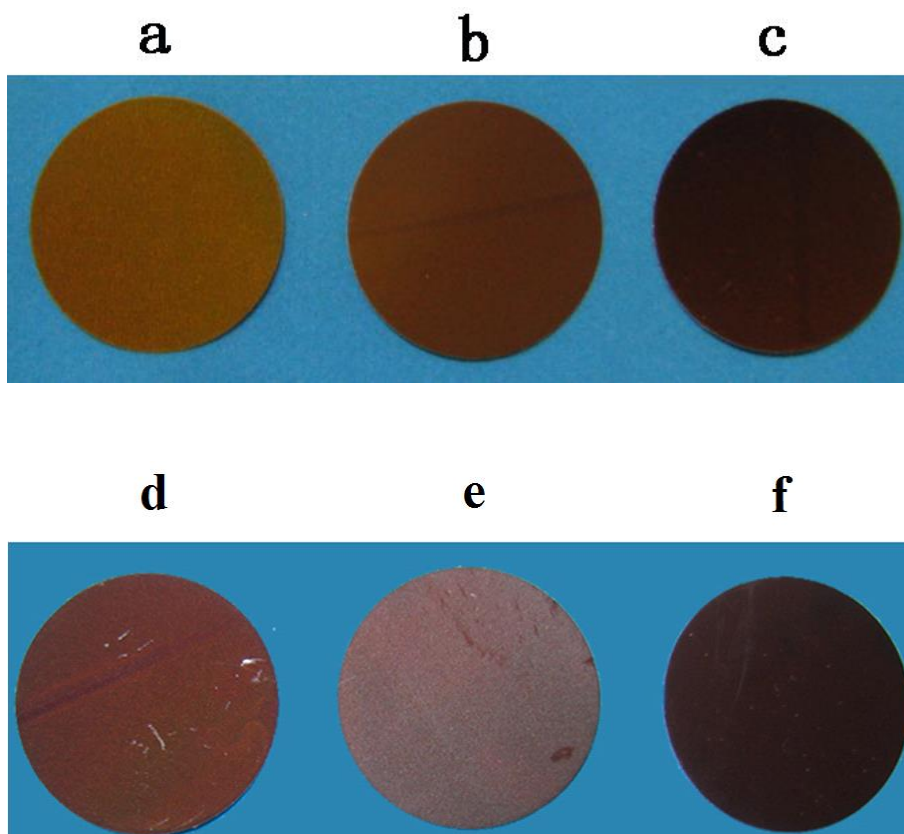


Figure S1: Views of anodic films grown on Fe foils in an ethylene glycol electrolyte containing 0,1M NH_4F and 2.5mL H_2O at 30 V for (a) and (d) 20min, (b) and (e) 30min, and (c) and (f) 60min, where (d), (e) and (f) are the samples annealed at 400 °C for 1h.

Highlights

1. Nanoporous anodic films on electroformed Fe foils were obtained by anodization at a safety voltage of 30 V.
2. Nanoporous $\text{Fe}_3\text{O}_4\text{-Fe}_2\text{O}_3/\text{Fe}$ composite foils were firstly prepared by anodizing and annealing of Fe foils.
3. Nanoporous $\text{Fe}_3\text{O}_4\text{-Fe}_2\text{O}_3/\text{Fe}$ composite anodes for Li-ion batteries present different electrochemical performances.

Graphical abstract

